01 Nov 2006

Humidification Factors from Laboratory Studies of Fresh Smoke from Biomass Fuels

D. E. Day
Missouri University of Science and Technology, day@mst.edu

J. L. Hand

C. M. Carrico

Guenter Engling

et. al. For a complete list of authors, see https://scholarsmine.mst.edu/matsci_eng_facwork/210

Humidification factors from laboratory studies of fresh smoke from biomass fuels

D. E. Day,[1] J. L. Hand,[1] C. M. Carrico,[2] Guenter Engling,[2,3] and W. C. Malm[4]

Received 21 February 2006; revised 25 May 2006; accepted 9 August 2006; published 16 November 2006.

[1] Measurements of smoke aerosol humidification factors were performed in a laboratory for different biomass fuel types and burn conditions. Two nephelometers simultaneously measured dry and humidified light scattering coefficients ($b_{sp(\mathrm{dry})}$ and $b_{sp(\mathrm{RH})}$, respectively), providing the first observations of the temporal evolution of the humidification factor ($f(\mathrm{RH}) = b_{sp(\mathrm{RH})}/b_{sp(\mathrm{dry})}$) for fresh (minutes-old) smoke. Hygroscopic characteristics of the smoke aerosols varied with fuel type and fire conditions, with the mean $f(\mathrm{RH})$ ranging from 1.01 to 1.95 for fresh minutes-old smoke for the relative humidity (RH) range of 70–94%. These $f(\mathrm{RH})$ values exhibited temporal variability, with some fuels alternating from hygroscopic to nonhygroscopic within minutes. Humidograms were also obtained, demonstrating that smoke from different fuels begins to take up water at different RH values. Humidification factors for hour-old smoke ranged from 1.10 to 1.51 for RH > 90%. Finally, light-absorbing carbon mass measured with a multiwavelength aethalometer demonstrated different spectral responses as a function of fuel type. These laboratory experiments demonstrate the complexity of smoke hygroscopicity from young fires and are essential for understanding the radiative effects of biomass burning in the ambient atmosphere.

Citation: Day, D. E., J. L. Hand, C. M. Carrico, G. Engling, and W. C. Malm (2006), Humidification factors from laboratory studies of fresh smoke from biomass fuels, *J. Geophys. Res.*, *111*, D22202, doi:10.1029/2006JD007221.

1. Introduction

[2] Estimates of radiative properties of biomass smoke depend on a complicated array of aerosol properties such as composition, hygroscopicity, particle size, and shape. All of these properties can vary depending on the type of biomass fuel, the intensity and combustion phase of the fire (e.g., flaming versus smoldering), as well as the age and degree of processing of the smoke. Biomass burning aerosol properties typically have been estimated from ambient observations of smoke plumes or regional smoke hazes (for a comprehensive review of biomass burning aerosols, see the review articles by *Reid et al.* [2005a, 2005b, and references therein]). Understanding the complicated properties of smoke aerosols from ambient measurements is hampered by the fact that fuel type, fuel moisture, flame conditions, smoke age, and mixing characteristics with background aerosols are generally unknown. Investigating the relationships between smoke aerosol properties and emissions requires studying the emissions of particulates at the fire source, preferably under controlled conditions. These types of investigations have motivated the laboratory studies of smoke aerosol properties from known biomass fuels and fire conditions [e.g., *Turn et al.*, 1997; *Christian et al.*, 2003; *Chen et al.*, 2006; *Engling et al.*, 2006]. To the extent of our knowledge, none of these studies has included direct measurements of the hygroscopic properties of young smoke.

[3] An important component for estimating the radiative effects of biomass smoke aerosols is the water uptake of the fresh and aged smoke particles. This effect is often quantified as GF, the change in particle size (D_p) with changing relative humidity (RH) ($\mathrm{GF} = D_{p(\mathrm{RH})}/D_{p(\mathrm{dry})}$) [e.g., *Cocker et al.*, 2001]. However, the uptake of water results in more than just changes in particle size; it also changes particle mass, composition, shape, morphology and optical properties. The change in particle light scattering properties as a function of RH is quantified as the humidification factor ($f(\mathrm{RH})$) and is defined as the light scattering coefficient of humidified aerosols ($b_{sp(\mathrm{RH})}$) divided by the light scattering coefficient of dry aerosols ($b_{sp(\mathrm{dry})}$). The humidification factor is a function of particle composition, hygroscopicity, size, and (to a lesser extent) shape, and has important implications for correctly estimating regional haze effects and climate forcing due to biomass burning. When estimating the effects of water uptake on particles, GF refers to only the change in particle size, while $f(\mathrm{RH})$ refers to changes in particle scattering properties. Furthermore, $f(\mathrm{RH})$ is inherently dependent on the effective cross section of the particle. To illustrate, pure ammonium sulfate par-

[1]Cooperative Institute for Research in the Atmosphere, Colorado State University, Fort Collins, Colorado, USA.
[2]Department of Atmospheric Science, Colorado State University, Fort Collins, Colorado, USA.
[3]Now at Research Center for Environmental Changes, Academia Sinica, Taipei, Taiwan.
[4]National Park Service, Cooperative Institute for Research in the Atmosphere, Colorado State University, Fort Collins, Colorado, USA.

0148-0227/06/2006JD007221

Table 1. Published Values of Biomass Burning Humidification Factors (f(RH)) Using Nephelometery[a]

f(RH) Range	RH(%) Humid/Dry	Fire Type	Location/Fuel	Instrument Platform	λ, nm	Reference
1.01–1.51	80/30	plume and regional haze	Brazil/Cerrado and pasture/forest	aircraft	550	*Kotchenruther and Hobbs* [1998]
1.1–1.7	80/20	flame and smoldering	North Australia/wooded savannah	aircraft	530	*Gras et al.* [1999]
1.2–2.1	80/20	smoldering, haze	Indonesia/rain forest, peat deposit	aircraft	530	*Gras et al.* [1999]
1.44 ± 0.02	80/30	ambient aged heavy smoke	African savannah	aircraft	550	*Magi and Hobbs* [2003]
1.66 ± 0.08	80/30	plumes within 10 min of emission	African savannah	aircraft	550	*Magi and Hobbs* [2003]
1.1–1.2	80–85/10–15	aged regional smoke/haze	Yosemite National Park, California (Oregon fires)	ground-based	530	*Malm et al.* [2005]
1.60 ± 0.20	85/40	aged regional smoke	Gosan, Korea (Russian and North Korean fires)	ground-based	550	*Kim et al.* [2006]
1.01 ± 0.05–1.76 ± 0.05	75–80/10	fresh minutes-old	laboratory/midlatitude forest fuels	laboratory	530	this study
1.10 ± 0.05–1.51 ± 0.05	~92/10	fresh hour-old	laboratory/midlatitude forest fuels	laboratory	530	this study

[a]The wavelength (λ) corresponds to the nephelometer measurement.

ticles with a mean diameter of 0.2 μm and a geometric standard deviation of 2.2 correspond to a GF of 1.5 at RH = 80%, while f(RH) $\approx$ 2.9. Typically, f(RH) is estimated empirically by measurements of light scattering coefficients performed under humidified and dried conditions; however, the reference or dry RH at which f(RH) is reported varies from study to study. In this study "dry" is defined as RH$\approx$10%, and humidified RH values range from 75 to 80% but in some cases are as high as mid-90%.

[4] Conflicting results from the few studies that report measured f(RH) factors in ambient smoke plumes emphasize the need for further measurements. Some of these studies are reviewed by *Reid et al.* [2005b] and are summarized in Table 1. For example, *Kotchenruther and Hobbs* [1998] obtained aircraft measurements of f(RH) values in the dry season in Brazil ranging from 1.01 to 1.51 with higher values observed for regional haze (aged conditions). In contrast, aircraft measurements performed by *Magi and Hobbs* [2003] in southern Africa suggest that aged smoke corresponds to lower f(RH) values, with similar values observed for ~hour-old smoke as for heavily aged smoke. Smoke sampled in association with regional haze could be mixed significantly with ambient inorganic aerosols, affecting the hygroscopic growth. Composition data would assist in investigating the role of background aerosols but were not reported as part of these studies. Ground-based measurements of f(RH) for aged (days-old) smoke in Yosemite National Park, California, were also very low (1.1–1.2) and increased strongly as the ratio of smoke organic carbon mass to ammonium sulfate mass decreased, showing that the effects of mixing with ambient aerosols are important [*Malm et al.*, 2005]. *Kim et al.* [2006] measured an f(RH) of 1.6 ± 0.20 corresponding to aged biomass smoke in Korea that was associated with higher organic carbon concentrations and lower sulfate mass fractions. Aircraft measurements performed by *Gras et al.* [1999] showed very different f(RH) factors for smoke from north Australian savannah fires (1.37) compared to peat fires in Indonesia (1.65), suggesting fuel composition played an important role in the smoke hygroscopicity. The variability of f(RH) values listed in Table 1 could be due to experimental or platform differences, biomass fuel type, location, flame conditions, mixing with ambient inorganic aerosols, or processing in the atmosphere (age). Constraining the range of estimates of f(RH) requires performing measurements under controlled conditions. Our study specifically addresses this need and is unique in that we report hygroscopic properties of young smoke (minutes- to hour-old) from known fuels and controlled burn conditions.

[5] Finally, light absorption characteristics of smoke were measured with a multiwavelength (λ) aethalometer to investigate the spectral light absorption of biomass fuels. Historically, light absorption by aerosols is assumed to be due to black carbon (soot) that has a spectral dependence corresponding to λ^{-1}, although early work demonstrates that organic compounds in biomass smoke do absorb shorter wavelength radiation [e.g., *Patterson and McMahon*, 1984]. Whether spectrally absorbing organic compounds are typically present in young biomass smoke and whether different fuels exhibit varying amounts of spectral absorption are investigated as a part of this study.

2. Experimental Methods

[6] The measurements were conducted at the United States Forest Service Rocky Mountain Research Station Fire Sciences Laboratory in Missoula, Montana, from 19 to 26 November 2003. This facility includes a burn chamber with a floor area of approximately 12.5 m by 12.5 m and a height of about 18 m. Two different experimental techniques were used to sample smoke. The first set of experiments involved sampling smoke aerosols through a stack and diluting the smoke with nitrogen gas. The second set of experiments was conducted by allowing the smoke to disperse throughout the chamber from which instruments sampled directly without dilution.

[7] The first set of experiments (referred to as "stack" burns) was designed to investigate emission characteristics of various fuel types [*Chen et al.*, 2006; *Engling et al.*, 2006]. A measured quantity of biomass, generally 250 grams, was burned on a continuously weighed platform situated under a stack. Unfiltered ambient air from outside the building was blown into the chamber, creating a slight overpressure inside the chamber. Thus smoke generated

during the stack burns was entrained in the stack flow, exiting the chamber through a vent above the stack. Instruments were situated on a hanging scaffold approximately 15 m above the chamber floor and plumbed directly to the stack. Smoke samples at this height have had sufficient time to cool and become well mixed [*Goode et al.*, 1999]. The burn platform also could be angled, resulting in a heading fire (fuel burning uphill) or a backing fire (fuel burning downhill), depending on whether the bottom or top of the fuel pile was ignited. Generally, three heading fires and three backing fires for each fuel type were burned. Although care was taken in sample preparation to achieve homogeneous piles, invariably each pile contained differing amounts of leaves and stems, and the thickness of woody material varied, resulting in slightly different burn characteristics. Smoke from stack burns was generally produced over periods of 4–8 min, depending on fuel type. For these experiments we report only the humidification factor of the aerosol.

[8] The second set of experiments involved allowing smoke from each burn to fill the entire chamber (referred to as "chamber" burns). These experiments were designed for instruments requiring longer sampling periods. Similar quantities of fuel as during the first set of experiments were burned on a flat platform situated in the middle of the chamber. The fire was ignited and then allowed to extinguish naturally. Instruments sampled smoke from the room directly without dilution for approximately two hours per burn. This sampling time also allowed for slowly ramping RH to obtain humidograms (f(RH) as a function of RH), thus observing the RH of initial water uptake. Aethalometer measurements of light-absorbing carbon mass were also performed as part of these experiments.

[9] Several types of biomass fuels were burned during these experiments, most reflecting midlatitude forest origins. White pine needles, ponderosa pine needles, African savannah grass, and sage brush were used in the stack burns. Sage brush, poplar, ponderosa pine wood and needles, cottonwood, oak, and Alaskan floor duff (forest litter and decayed organic material) were used in the chamber burns. Data for ponderosa pine wood and needles are only available from the aethalometer because of instrument malfunction. All of the fuels were stored in a dry location prior to burning and assumed to have low moisture contents, with the exception of Alaskan floor duff, which contained some moisture. Differences in moisture content likely affect burn temperatures and smoke emissions.

2.1. Nephelometer Measurements and Uncertainty

[10] Two Radiance Research M903 nephelometers (Radiance Research Inc, Seattle, Washington) measured light scattering coefficients (b_{sp}) at a wavelength of 530 nm. The nephelometers sampled through identical lines that were connected to a $PM_{2.5}$ URG cyclone (URG, Chapel Hill, North Carolina). Relative humidity and temperature were monitored at the entrance and exit of the nephelometers using Rotronic Hygroclip sensors (Rotronic Instruments (UK) LTD, West Sussex, UK) with a reported accuracy in relative humidity of ±1.5%RH at 23°C. The probe accuracy was checked against a Kaymont Model 2000 humidity generator (Kaymont, Huntington Station, New York) with reference probes calibrated with laboratory standard salt solutions. The Rotronic Hygroclip sensors were within ±1%RH of the standard at 25%, 85% and 95% relative humidity. We estimate our uncertainty in RH to be ±3% to include uncertainties in relative humidity inside the nephelometer due to temperature variations (≈0.5°C) inside the nephelometer. During both sets of experiments, dry light scattering coefficients ($b_{sp(\mathrm{dry})}$) were measured for RH < 10%. During the stack burns the humidified scattering coefficients ($b_{sp(\mathrm{RH})}$) corresponded to RH > 75%. For the chamber burns RH was ramped over a range of values up to 90% or higher in some cases. Sample RH was controlled using Perma Pure diffusion tubes (Perma Pure LLC, Toms River, New Jersey). Aerosol light scattering coefficients, sample RH, and sample temperature were logged at 5-s time intervals. The nephelometers were calibrated daily with clean filtered air and SUVA (HFC 134a) span gas.

[11] Corrections due to particle losses in the tubing were not applied to the nephelometer data because the instruments sampled from identical tubing, and in the calculation of f(RH), those losses cancel. However, under humidified conditions the Perma Pure tube could cause additional losses, but, as discussed below, these losses were within our measurement uncertainty. Corrections for angular truncation effects were not included because model calculations for size distributions in the $PM_{2.5}$ range were considered minimal (approximately −1%, J. V. Molenar, personal communication, 1997). Therefore the uncertainties in b_{sp} were estimated by propagating errors (one standard deviation) derived from calibration data. Other issues besides calibration affect total uncertainty, such as the accuracy of pressure and temperature sensors; however, these instrumental errors also affect calibration measurements and would contribute to any variations observed in the calibration data. Uncertainties ranged from 5% to 20%, depending on whether the b_{sp} signal was large (∼500 Mm^{-1}) and dominated by the SUVA calibration, or small (∼5 Mm^{-1}) and dominated by the clean filtered air calibration, respectively. On average the uncertainty in b_{sp} from each nephelometer was estimated to be approximately ±5% for the 5-s sampling frequency.

[12] To assess whether the calibration uncertainties were realistic and accounted for differences observed in b_{sp}, Montana prairie grass and Alaskan floor duff were burned in the stack under dry (RH < 20%) conditions. Data from the two nephelometers for these two fuels are shown in Figure 1 with error bars reflecting the calibration uncertainties, and the comparison suggests that the calibration uncertainties are accounting for the differences seen in the measurements. No biases were observed between the data that would reflect other unaccounted for sources of uncertainty. An ordinary linear regression in the data resulted in a slope of 1.03 ± 0.0009, intercept of −3.09 ± 0.201 Mm^{-1}, and high correlation coefficient (R^2 = 0.999). The mean absolute value and one standard deviation of the difference in b_{sp} are 5.6 Mm^{-1} and 6 Mm^{-1}, respectively, while the difference ranged from 0.0069 to 54 Mm^{-1}. The uncertainty in f(RH) was computed by propagating the calibration uncertainties in b_{sp} and was approximately ±0.05 on average for the data set. Using unpublished background soluble ion aerosol composition data from the study, we estimate an upper limit contribution of background aerosols to f(RH) (from the unfiltered ambient air used to flush the chamber between burns) to be approximately 0.02. Although back-

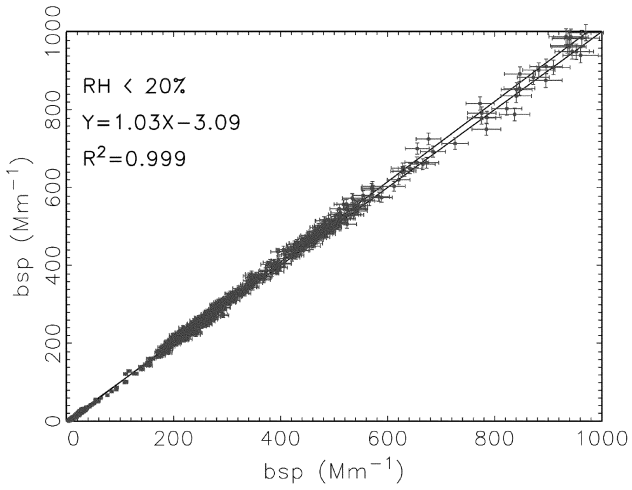

Figure 1. Comparison of dry (RH < 20%) light scattering coefficients (b_{sp}) from nephelometer measurements (530 nm wavelength) for Montana prairie grass and Alaskan floor duff. The 1:1 line and the line representing the linear regression results are shown on the figure. Error bars represent uncertainty due to the calibration.

ground aerosols could be contributing to f(RH), the effect is within our measurement uncertainty. As mentioned previously, additional particle losses due to the Perma Pure tube under humidified conditions could exist and would result in a depression of $b_{sp(\mathrm{RH})}$ relative to $b_{sp(\mathrm{dry})}$ for weak to nonhygroscopic particles. However, we did not observe any such decrease, indicating that the effect of these losses is within our measurement uncertainty. However, for hygroscopic particles the losses in the humidified Perma Pure tube may exist but would be difficult to detect because although the $b_{sp(\mathrm{RH})}$ signal is reduced, it still increases over $b_{sp(\mathrm{dry})}$. Given this possibility, the f(RH) values reported here may be an underestimation.

2.2. Aerosol Absorption

[13] Aerosol light absorption measurements were conducted with a seven wavelength (λ) aethalometer (Magee Scientific AE-31, Berkeley, California). The aethalometer reports light-absorbing carbon (LAC) mass by measuring light attenuation from particulates deposited on a quartz fiber filter [*Hansen et al.*, 1984]. The quartz fiber filter tape advances to a clean filter spot once the attenuation in a given wavelength channel has reached a nominal value during a measurement cycle. The aethalometer data were logged as 5-min averages. Minimum detection limits of the aethalometer were assumed to be around 70 ng m^{-3} at 880 nm [*Brown*, 2001]. We use the term "light-absorbing carbon" to reflect all types of carbonaceous aerosols that absorb light, and we use the term "black carbon" to refer to graphitic (soot-like) carbon particles. A λ^{-1} relation (i.e., wavelength-dependent mass absorption efficiency) allows for calculation of an equivalent light-absorbing carbon mass as a function of wavelength for λ = 370, 470, 520, 590, 660, 880, and 950 nm [e.g., *Bergstrom et al.*, 2001; *Kirchstetter et al.*, 2004]. Recent studies suggest that the aethalometer overpredicts LAC on a fresh filter and underpredicts LAC on a loaded filter because of multiple scattering effects [e.g., *Weingartner et al.*, 2003; *Arnott et al.*, 2005; *Schmid et al.*, 2005]. Without correcting for these effects, absorption coefficients derived from aethalometer data are semiquantitative, especially for highly absorbing particles. *Arnott et al.* [2005] point out that longer wavelength channels of the multiwavelength aethalometer are less affected by multiple-scattering effects compared to the shorter wavelength channels. Therefore both the concentration of LAC and its spectral dependence from uncorrected aethalometer data are subject to uncertainty. No corrections to the data based on these known issues were included here as we focused on the qualitative differences observed between the spectral variations in LAC mass for different fuel types.

3. Results

3.1. Humidification Factor (f(RH))

3.1.1. Stack Burns

[14] Although smoke from the stack burn experiments lasted only a few minutes, considerable differences in hygroscopic properties for different fuels were observed (see Table 2). The humidified nephelometer measurements were performed for RH values typically between 75% and 80%. Although the RH increased slightly throughout the duration of each burn, no burn experienced more than a 2% increase in sample RH for its duration. The mean f(RH) for each fuel type was computed by averaging all data from heading and backing burns, respectively. The RH values reported in Table 2 reflect the observed range for three

Table 2. Average Humidification Factors (f(RH)) From the Stack Burns[a]

			f(RH)			
Material	Fire Type	RH, %	Minimum	Maximum	Mean	Standard Deviation
White pine needles	H	75–80	0.85	1.29	1.02	0.076
White pine needles	B	75–80	0.86	1.31	1.01	0.080
Sage brush	H	75–80	0.89	2.41	1.39	0.376
Sage brush	B	71–80	0.86	3.03	1.76	0.497
African savanna grass	H	80–87	0.70	1.17	1.01	0.110
African savanna grass	B	71–84	0.72	1.34	1.07	0.118
Ponderosa pine needles	H	77–80	1.03	1.72	1.25	0.125
Ponderosa pine needles	B	79–81	0.91	1.99	1.50	0.198
Ponderosa pine needles	B	85–87	1.02	1.86	1.58	0.182
Ponderosa pine needles	B	94	1.32	2.95	1.95	0.355

[a]Heading fires are denoted as "H," backing fires are denoted as "B." The uncertainty in f(RH) is approximately ±0.05. Dry nephelometer measurements were performed for RH < 10% at a wavelength of 530 nm. The minimum, maximum, mean and one standard deviation are reported. Uncertainty in RH is approximately ±3% (RH percentage points).

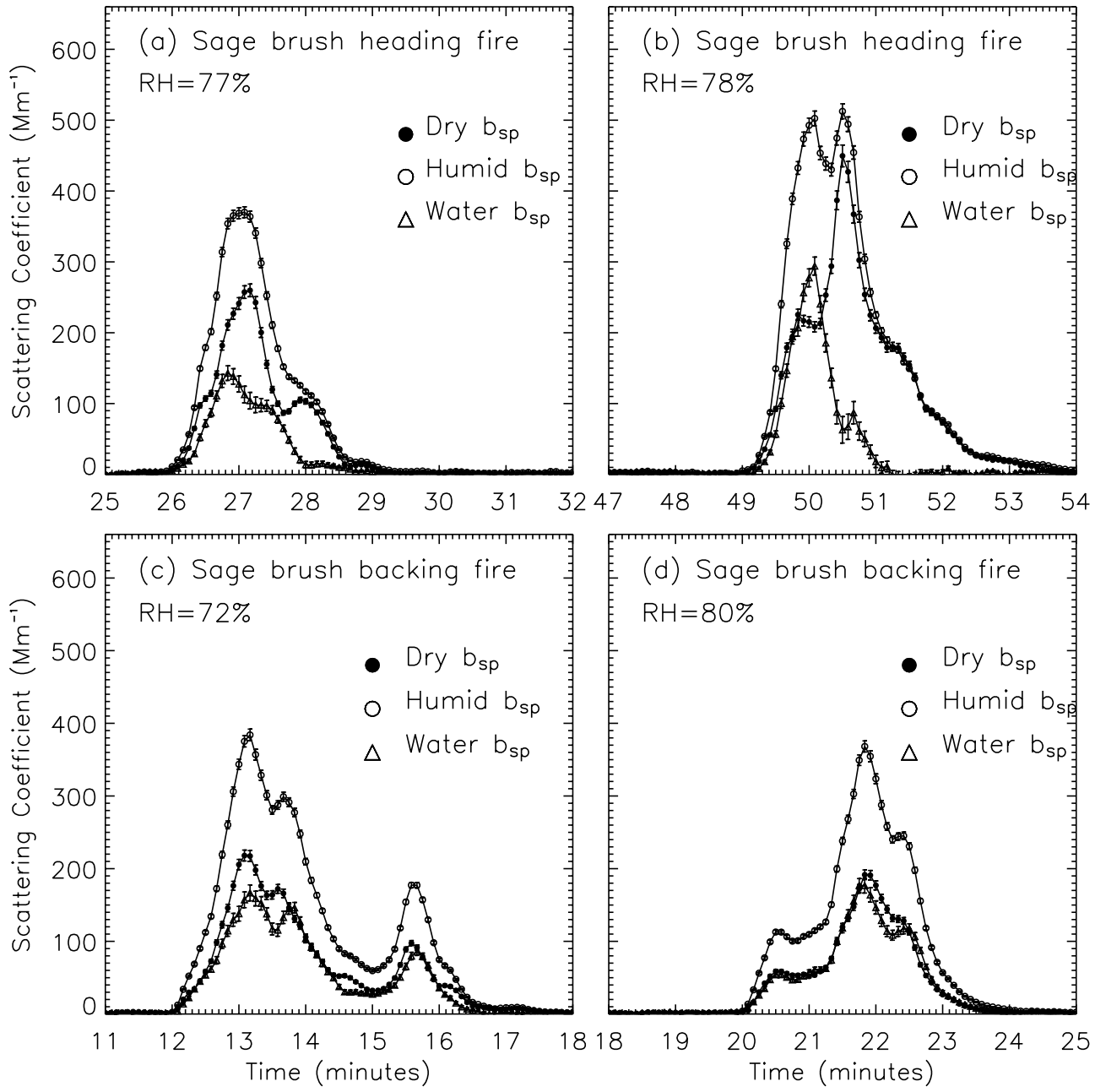

Figure 2. Timelines of light scattering coefficients (b_{sp}) corresponding to dry and humidified conditions and water ($b_{sp(\mathrm{RH})} - b_{sp(\mathrm{dry})}$) during stack burns of sage brush for (a and b) heading and (c and d) backing fires. The relative humidity (RH) of $b_{sp(\mathrm{RH})}$ is recorded on each plot. Dry measurements were performed for RH < 10%. The nephelometers are operated at a wavelength of 530 nm. Uncertainties in nephelometer data are shown as error bars, and the uncertainty in RH is approximately ±3%.

averaged burns. The range of RH values used in the stack burn experiments is at the limit of water uptake for many pure inorganic salts. For instance, ammonium nitrate deliquesces around 62%, while potassium chloride deliquesces at a higher RH of 84%. It is possible that water uptake would not be observed if the RH of deliquescence is higher for some of the smoke generated by the fuels used here. However, several researchers have reported continuous f(RH) as a function of RH for ambient measurements, suggesting a mixed aerosol (such as smoke) may not exhibit deliquescent behavior like pure salts do [e.g., *Im et al.*, 2001; *Malm et al.*, 2003, 2005; *Carrico et al.*, 2003, 2005].

[15] The lowest mean f(RH) (and one standard deviation) corresponded to white pine needles and African savanna grass. Within uncertainty, these fuels took up no significant amounts of water even when exposed to RH values up to 80%. In contrast, sage brush smoke was significantly hygroscopic (f(RH) = 1.39 and 1.76 for heading and backing fires, respectively), as was ponderosa pine needle smoke (1.25 and 1.50 for heading and backing fires, respectively). The mean f(RH) for ponderosa pine needles at RH = 94% was 1.95. The f(RH) for sage brush at 80% RH was 2.41 and 3.03 at 83% RH for the heading and backing fires, respectively.

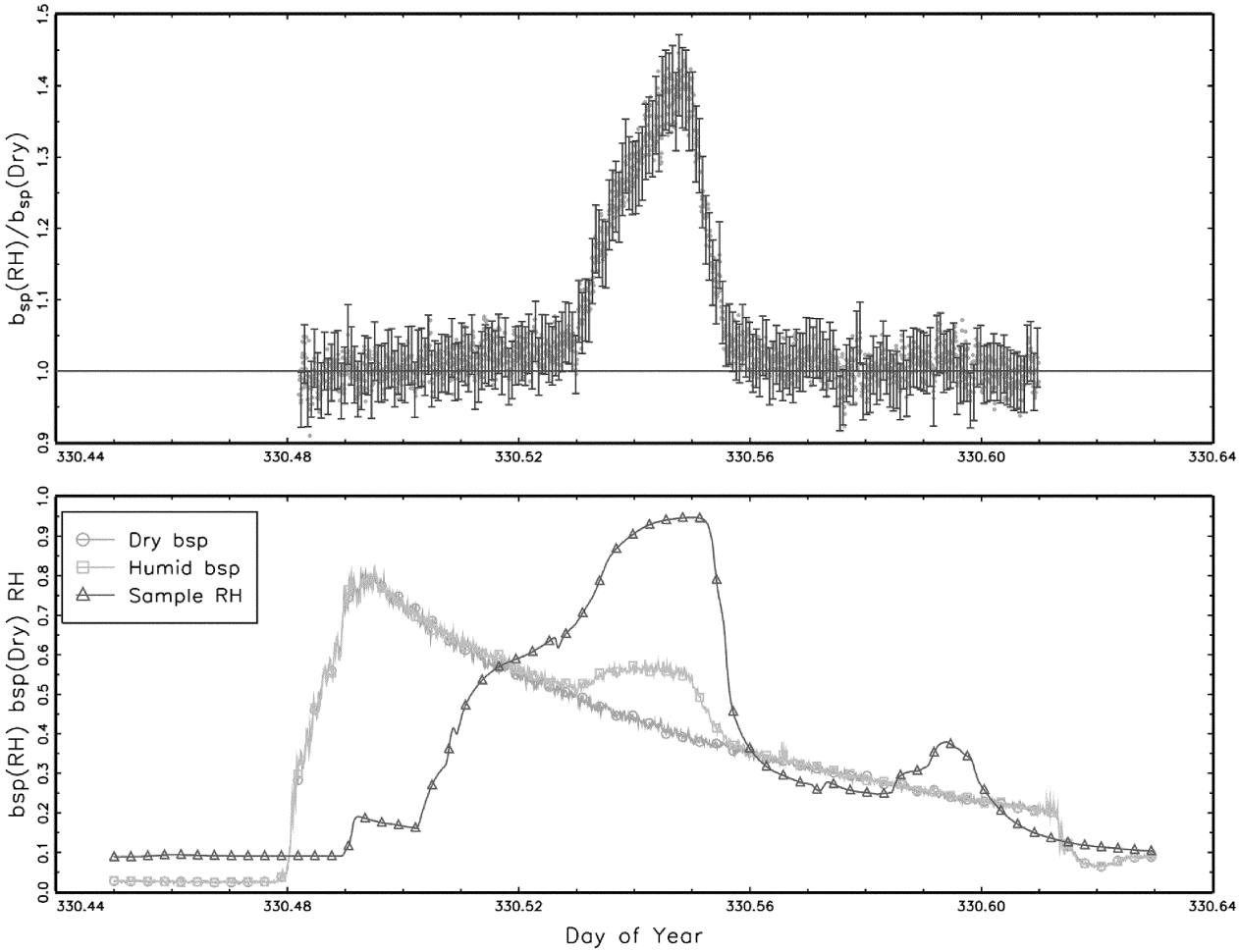

Figure 3. Timelines of the dry and humidified light scattering coefficients (b_{sp}) for sage brush during chamber burns. (top) Humidification factors (f(RH) = $b_{sp(RH)}/b_{sp(dry)}$) and (bottom) light scattering coefficients (b_{sp}/1000 Mm^{-1}). Humidified relative humidity (RH) is plotted as a fraction. Dry b_{sp} measurements were performed for RH < 10%. The uncertainties in f(RH) are plotted as error bars. The uncertainty in RH is approximately ±3%. Nephelometer measurements were performed at a wavelength of 530 nm.

[16] Temporal variations in f(RH) were observed over very short timescales. Timelines of $b_{sp(RH)}$, $b_{sp(dry)}$, sample RH, and the scattering coefficient due to water ($b_{sp(water)}$ = $b_{sp(RH)} - b_{sp(dry)}$) for two heading and backing sage brush fires are shown in Figures 2a–2d. The heading fires for sage brush were initially hygroscopic, but changed to nonhygroscopic minutes later (Figures 2a and 2b). In contrast, the backing fires appeared to be hygroscopic for the duration of the burn (Figures 2c and 2d). In fact, as seen in Table 2, the sage brush backing fires were significantly more hygroscopic compared to the heading fires. This behavior was also observed for smoke from ponderosa pine needles. However, African savanna grass and white pine needles demonstrated no significant differences in f(RH) for heading and backing conditions, nor were they significantly hygroscopic as already mentioned. The differences seen in the heading and backing fires were most likely due to differences in the intensity and combustion phase of the fires. During heading fires the flames spread uphill quickly, engulfing the entire pile of material in a high-intensity flame soon after ignition. In these types of fires all leafy and bark material were burned first, while the woody plant material burned last. During backing fires, the narrower flame zone moved downhill more slowly, increasing the residence time of the flame and causing the leafy and woody material to be burned simultaneously. The different burn conditions, especially for the heading fires, apparently led to rapid variations in the chemical composition of the aerosols, affecting their hygroscopicity. However, these differences were not observed for all fuel types. Whether the variations in observed f(RH) were a result of the fuel composition or due to rapid chemical and physical processes in the flame was not evident from these results.

3.1.2. Chamber Burns

[17] The smoke from the materials burned in the chamber generally lasted around two hours, while the concentration of aerosols decreased over this period because of deposition, and to a lesser extent, the removal of particulates from the chamber by various instruments. Between each burn the chamber was flushed with ambient unfiltered air. The RH in

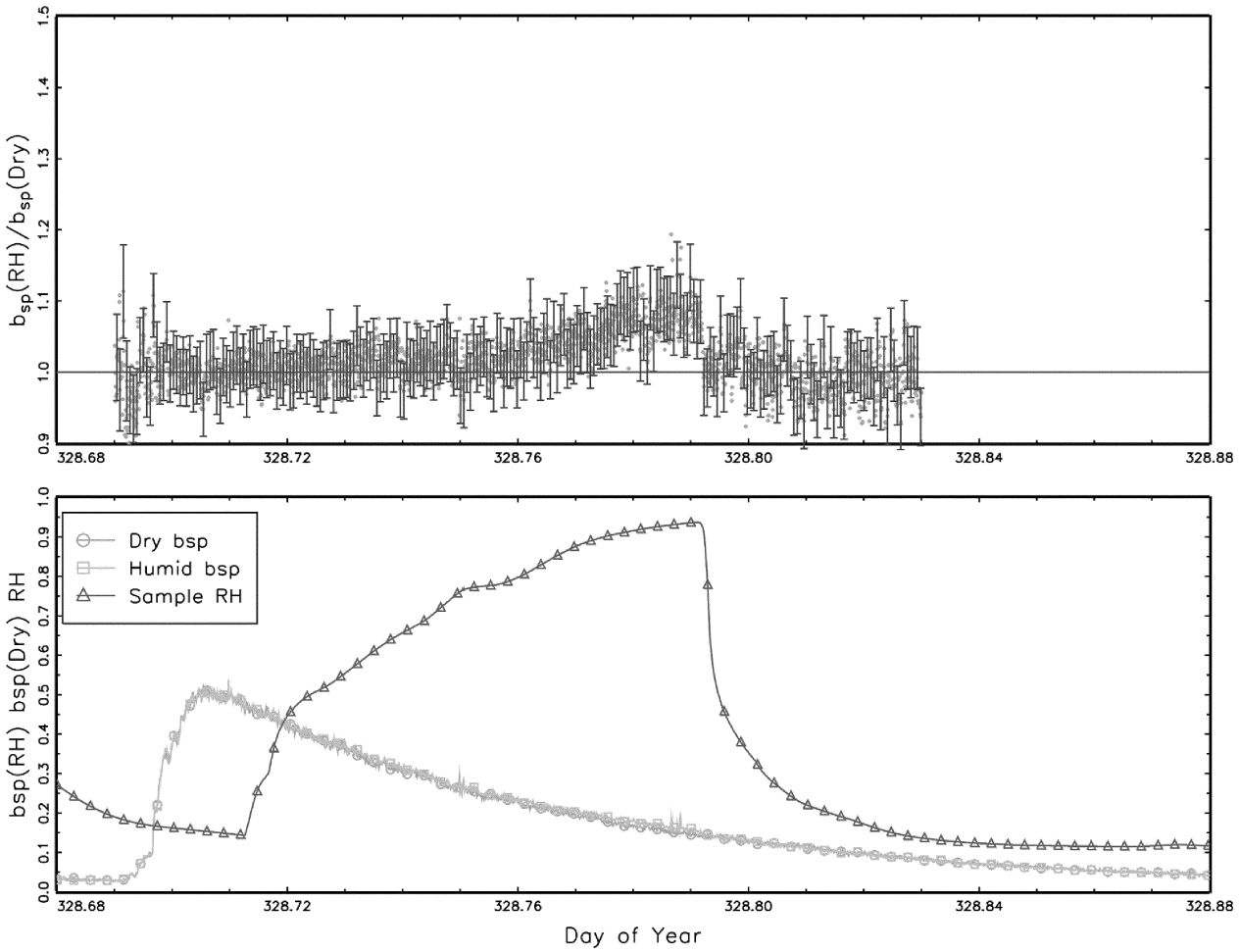

Figure 4. Timelines of the dry and humidified light scattering coefficients (b_{sp}) for cottonwood during chamber burns. (top) Humidification factors (f(RH) = $b_{sp(RH)}/b_{sp(dry)}$) and (bottom) light scattering coefficients (b_{sp}/1000 Mm^{-1}). Humidified relative humidity (RH) is plotted as a fraction. Dry b_{sp} measurements were performed for RH < 10%. The uncertainties in f(RH) are plotted as error bars. The uncertainty in RH is approximately ±3%. Nephelometer measurements were performed at a wavelength of 530 nm.

the first nephelometer was maintained below 10%, while the RH in the second nephelometer was slowly ramped from low to high values to obtain humidograms. Timelines of relative values of $b_{sp(RH)}$, $b_{sp(dry)}$ (scaled to fit the plot), sample RH (as a fraction), and f(RH) are shown in Figures 3 and 4 for sage brush and cottonwood, respectively. The decrease in light scattering coefficients over time reflects the removal of smoke from the chamber. Differences in f(RH) were observed as a function of fuel type, as seen by comparing Figures 3 and 4. Smoke aerosols from sage brush started to take up water between 65 and 70% RH, with f(RH) reaching a value of 1.30 for RH = 92%. When RH was decreased, f(RH) returned to a value of 1. In contrast, smoke aerosols from the burning of cottonwood showed only minimal uptake of water over the range of RH sampled (f(RH) = 1.13 at RH = 92%). Poplar smoke demonstrated the most hygroscopic behavior of the fuels burned, with water uptake initially occurring around an RH of 40–50%, and reaching f(RH) = 1.51 at an RH of 92%. Chestnut oak and Alaskan floor duff were nonhygroscopic to only minimally hygroscopic for RH values up of 92%. An overview of these results is provided in Table 3. Sage brush was the only material burned in both experiments and it is interesting to note that its average f(RH) values were similar for chamber and stack heading burns, but stack backing fires resulted in significantly higher f(RH) factors compared to the chamber burns, even though $b_{sp(RH)}$ was sampled at a higher RH during the chamber experiments (92%).

3.2. Aerosol Light Absorption

[18] Light absorption by fresh smoke aerosols was investigated using a multiple-wavelength (λ) aethalometer that measures light attenuation from particles deposited on a quartz fiber filter at seven wavelengths. The conversion applied by the manufacturer to obtain LAC mass concentrations includes the λ^{-1} spectral dependence of graphitic (or black) carbon often observed for soot particles [e.g., *Bergstrom et al.*, 2001; *Kirchstetter et al.*, 2004]. Thus, in

Table 3. Average Humidification Factors (f(RH)) From the Chamber Burns[a]

Material	RH at Initial Water Uptake, %	Mean f(RH) at RH
Sage brush	65–70	1.30 at 92%
Poplar	40–50	1.51 at 93%
Cottonwood	≈80	1.13 at 92%
Chestnut oak	≈75	1.19 at 92%
Alaskan floor duff	≈75	1.10 at 92%

[a]The uncertainty in f(RH) is approximately ±0.05. Dry nephelometer measurements were performed for RH < 10% at a wavelength of 530 nm. Uncertainty in RH is approximately ±3% (RH percentage points).

theory, when sampling small black carbon particles, the multiwavelength aethalometer is calibrated to output an equivalent mass of black carbon for all wavelengths, meaning that the mass concentrations from each wavelength channel should be equal if pure black carbon particles were the only absorbers on the filter.

[19] Organic carbon associated with aerosol particles produced from biomass burning previously has been reported to contribute to absorption in the UV and blue spectral regions [e.g., *Patterson and McMahon*, 1984; *Guyon et al.*, 2003; *Kirchstetter et al.*, 2004; *Hand et al.*, 2005; *Hoffer et al.*, 2006]; however, with the exception of the experiments by *Patterson and McMahon* [1984], these measurements were made in ambient conditions where the fire type and biomass fuels were generally unknown. We investigate the spectral variation of LAC mass from the aethalometer data to determine whether any additional light absorption by organic carbon compounds occurs as a function of fuel type. Because the absorption efficiencies of organic carbon are highly variable, the LAC mass reported by the aethalometer at short wavelengths is not a quantitative measure of organic carbon mass, but is interpreted as a qualitative indication of light absorption by organic carbon, although it is conceivable that other species could also contribute (e.g., hematite).

[20] A timeline of aethalometer LAC concentrations (μg m^{-3}) is presented for a single tape-advance cycle for sage brush smoke in Figure 5a. The decreasing concentrations in time were due to the diminishing smoke concentrations in the chamber, but also included the effects of multiple scattering of particles in the filter matrix when sampling light-absorbing aerosol. The decrease of LAC concentrations with time was attributed to the overprediction of LAC on a fresh filter and underprediction on a loaded filter, as reported by others for relatively constant aerosol sources [e.g., *Weingartner et al.*, 2003; *Arnott et al.*, 2005]. It is clear from Figure 5a that each channel was affected differently,

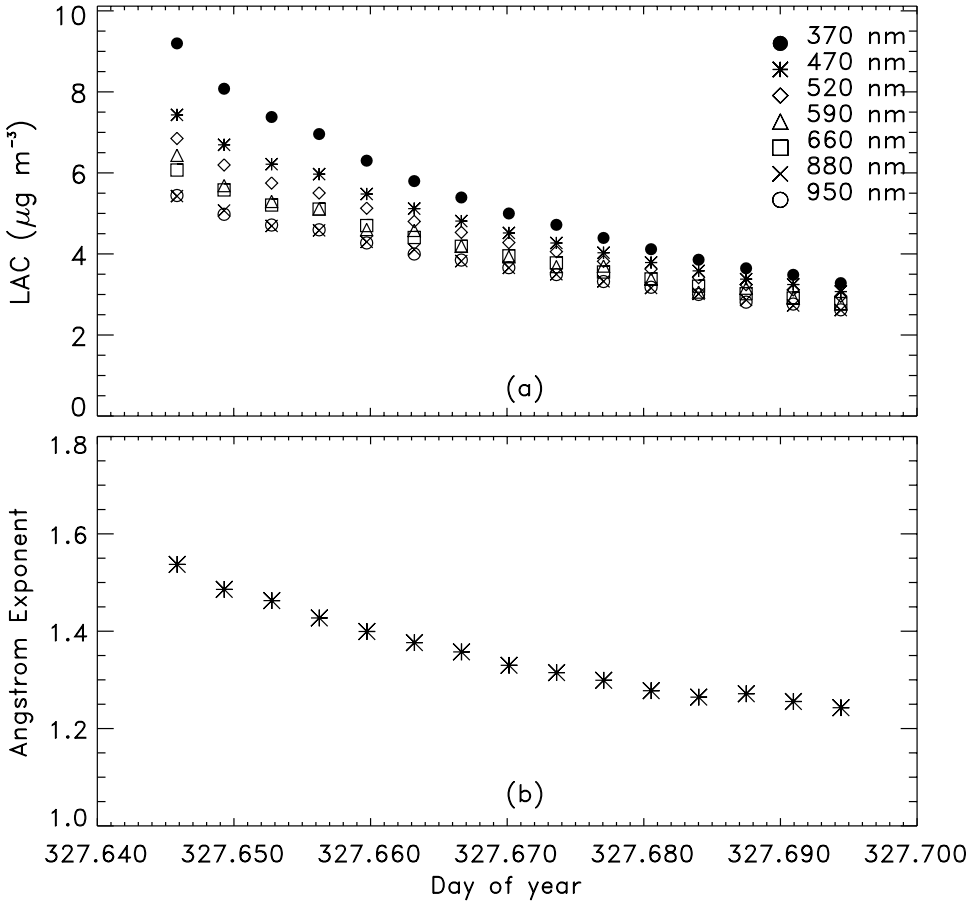

Figure 5. (a) Timeline of sagebrush light-absorbing carbon (LAC) concentrations from chamber burns using a seven-wavelength aethalometer. (b) Pseudo-Ångstrom exponent computed from LAC data in Figure 5a. A value of 1 corresponds to a λ^{-1} spectral dependence.

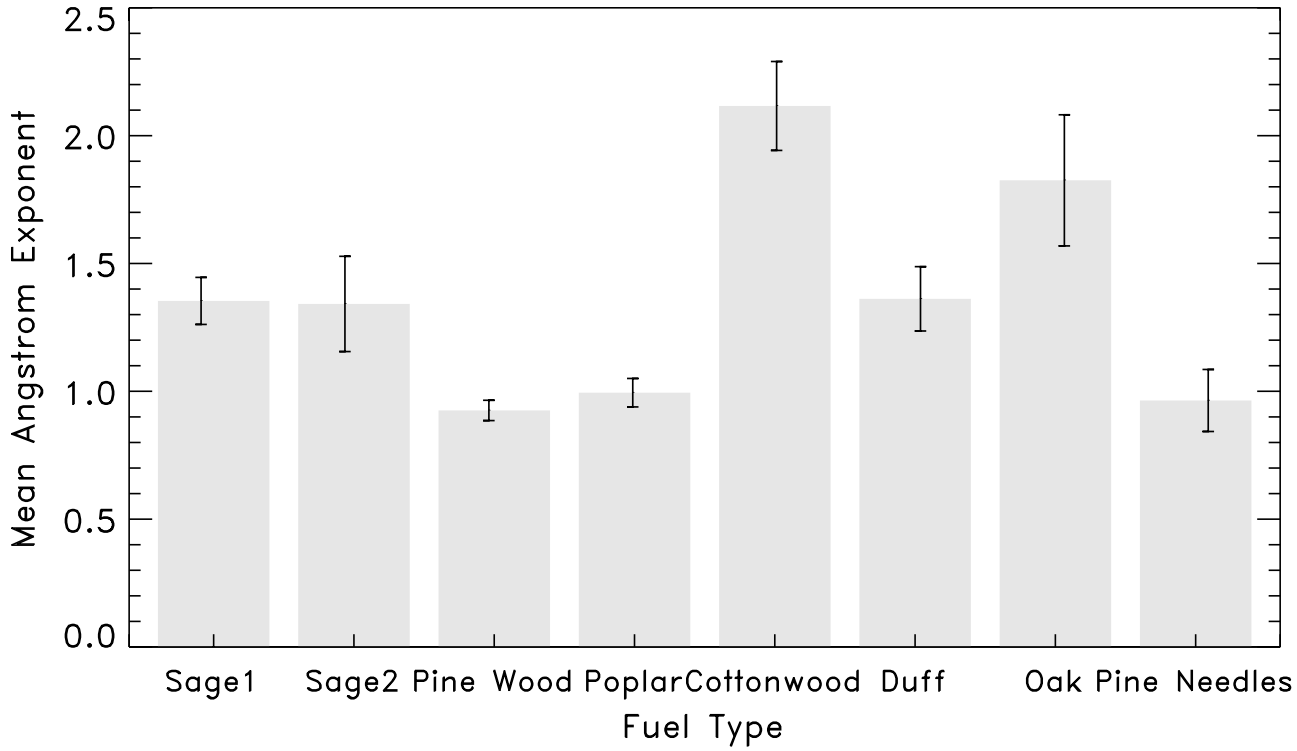

Figure 6. Mean pseudo-Ångstrom exponent as a function of fuel type. Error bars denote one standard deviation in the mean. The fuel types are sage brush (burn 1 and burn 2), ponderosa pine wood, poplar, cottonwood, Alaskan floor duff, oak, and ponderosa pine needles. A value of 1 corresponds to a λ^{-1} spectral dependence.

with longer wavelength channels affected less than the shorter wavelength channels, as discussed by *Arnott et al.* [2005].

[21] The timeline in Figure 5a also indicates a clear spectral dependence whereby the short wavelength channel LAC concentrations were higher than longer wavelength channel concentrations. This spectral variation suggested stronger absorption in the UV than the λ^{-1} relation accounts for, probably due to additional light absorption by organic carbon, as discussed earlier. As a means to compare the spectral variation from different biomass fuels, a pseudo-Ångstrom exponent was calculated using the following equation:

$$\mathrm{LAC} = \mathrm{k}^{*}\lambda^{-\alpha} \tag{1}$$

where LAC is the mass concentration reported by the aethalometer, k is a constant, λ is the wavelength of light, and α is the pseudo-Ångstrom exponent. Estimates of α were adjusted to include the λ^{-1} dependence so that α is directly comparable to other reported estimates (as reviewed by *Kirchstetter et al.* [2004]). A timeline of α for sage brush smoke aerosol for a single tape-advance cycle is shown in Figure 5b. Note the decrease in α over time. This temporal variation reflects the wavelength dependence of the multiple scattering effects as the filter load increases (as seen in Figure 5a) and perhaps changes in the organic speciation of the smoke aerosols. We do not attempt to correct for the instrumental artifacts because we have no independent measurement of aerosol light absorption, and aerosol concentrations were not constant. Instead, we average α over a single cycle within the burn duration to qualitatively compare the spectral response from different forest fire fuels. The results for all types of biomass are shown in Figure 6. One standard deviation in the mean is included in Figure 6 to reflect the variation observed. Ponderosa pine needles, wood, and poplar demonstrated very little spectral response beyond what is expected for black carbon (α = 1). Smoke from sage brush demonstrated a higher spectral dependence with $\alpha \sim 1.4$. Replicate burns with sage brush suggest these estimates were reproducible (see Figure 6). Estimates for Alaskan floor duff were comparable to sage brush ($\alpha \sim 1.4$), indicating some light absorption by organic carbon. The largest spectral response was observed for cottonwood ($\alpha \sim 2.1$) and oak ($\alpha \sim 1.8$), and was considerably higher than what would be expected for pure black carbon particles.

4. Summary

[22] Measurements of fresh young (minutes-old) and pre-aged (hour-old) laboratory-generated smoke aerosols from biomass fuels demonstrated considerable differences in hygroscopic properties as characterized by nephelometry. Humidification factors (f(RH)) indicated that the water uptake of smoke alternated from hygroscopic to nonhygroscopic within minutes, and varied significantly with fuel type and burn conditions (e.g., heading versus backing fires). Mean humidification factors for fresh minutes-old smoke ranged from 1.02 to 1.95 over relative humidity

ranges of 75–94% depending on the fuel type and fire condition. Differences observed in the hygroscopic properties were probably due to the variations in the fire intensity and combustion phase (flaming versus smoldering), as well as differences in fuel composition, although we lack observations to reveal the processes responsible. Somewhat lower f(RH) factors were observed for fresh pre-aged (hour-old) smoke compared to young (minutes-old) smoke, with pre-aged smoke values ranging from 1.10–1.51 for RH near 90%. The ranges of f(RH) observed for pre-aged smoke mainly reflect fuel type, as the fire conditions were similar for each burn, although the combustion phases and efficiencies may have differed. The RH of initial water uptake also varied as a function of fuel type, ranging from 40 to 50% for poplar to around 80% for cottonwood. Our lower values of f(RH) for pre-aged smoke are consistent with the results reported by *Malm et al.* [2005] and *Magi and Hobbs* [2003] for aged (processed) smoke measured in the ambient atmosphere.

[23] Multiwavelength aethalometer measurements of LAC mass concentrations suggested that fresh smoke from some fuels was spectrally absorbing to a greater extent than predicted for black carbon, indicating that organic carbon was contributing to light absorption. However, other fuels demonstrated no such spectral variation beyond a λ^{-1} relationship. For example, sage brush, cottonwood and Alaskan floor duff smoke absorbed more UV and visible radiation than expected for pure black carbon soot, while poplar, ponderosa pine wood and pine needle smoke did not demonstrate enhanced light absorption. The spectral absorption of organic compounds in smoke appeared to be more a function of fuel type and burn conditions than atmospheric processing, at least for our observations.

[24] The results reported here for fresh smoke, obtained under laboratory settings with known biomass fuels and burn conditions, are important for understanding the range of f(RH) results reported for ambient measurements (see Table 1). Even under controlled settings, our range of results reflects the f(RH) estimates obtained in the ambient atmosphere under a variety of experimental conditions, global fire locations, fire intensity and phase, and atmospheric processing. Although we observed that a variety of fuel types and fire conditions resulted in a range of f(RH) values, undoubtedly the fire intensity and combustion phase also affect f(RH). Clearly, more research is needed to fully understand the complicated nature of biomass combustion processes that contribute to the uncertainties in smoke radiative properties.

[25] **Acknowledgments.** We gratefully acknowledge the USFS Fire Science Laboratory staff, including Emily Lincoln, Ron Babbitt, Ron Susott, Cyle Wold, and Ted Christian, for their valuable support and assistance during the study. Funding was provided by the U. S. National Park Service.

References

Arnott, W. P., K. Hamasha, H. Moosmuller, P. J. Sheridan, and J. A. Ogren (2005), Towards aerosol light-absorption measurements with a 7-wavelength aethalometer: Evaluation with a photoacoustic instrument and 3-wavelength nephelometer, *Aerosol. Sci. Technol.*, *39*, 17–29.

Bergstrom, R. W., P. B. Russell, and P. Hignett (2001), Wavelength dependence of the absorption of black carbon particles: Predictions and results from the TARFOX experiment and implications for the aerosol single scattering albedo, *J. Atmos. Sci.*, *59*, 567–577.

Brown, S. G. (2001), Characterization of carbonaceous aerosol during the Big Bend Regional Aerosol and Visibility Observational Study, M. S. thesis, Colo. State Univ., Fort Collins.

Carrico, C. M., P. Kus, M. J. Rood, P. K. Quinn, and T. S. Bates (2003), Mixtures of pollution, dust, sea salt, and volcanic aerosol during ACE-Asia: Radiative properties as a function of relative humidity, *J. Geophys. Res.*, *108*(D23), 8650, doi:10.1029/2003JD003405.

Carrico, C. M., S. M. Kreidenweis, W. C. Malm, D. E. Day, T. Lee, J. Carrillo, G. R. McMeeking, and J. L. Collett Jr. (2005), Hygroscopic growth behavior of a carbon-dominated aerosol in Yosemite National Park, *Atmos. Environ.*, *39*, 1393–1404.

Chen, L.-W. A., H. Moosmüller, W. P. Arnott, J. C. Chow, J. G. Watson, R. A. Susott, R. E. Babbitt, C. E. Wold, E. N. Lincoln, and W. M. Hao (2006), Particles emissions from laboratory combustion of wildland fuels: In situ optical and mass measurements, *Geophys. Res. Lett.*, *33*, L04803, doi:10.1029/2005GL024838.

Christian, T. J., B. Kleiss, R. J. Yokelson, R. Holzinger, P. J. Crutzen, W. M. Hao, B. H. Saharjo, and D. E. Ward (2003), Comprehensive laboratory measurements of biomass-burning emissions: 1. Emissions from Indonesian, African and other fuels, *J. Geophys. Res.*, *108*(D23), 4719, doi:10.1029/2003JD003704.

Cocker, D. R., N. E. Whitlock, R. C. Flagan, and J. H. Seinfeld (2001), Hygroscopic properties of Pasadena, California, aerosol, *Aerosol Sci. Technol.*, *35*(2), 637–647.

Engling, G., P. Herckes, S. M. Kreidenweis, W. C. Malm, and J. L. Collett Jr. (2006), Composition of the fine organic aerosol in Yosemite National Park during the 2002 Yosemite Aerosol Characterization Study, *Atmos. Environ.*, *40*, 2959–2972.

Goode, J. G., R. J. Yokelson, R. A. Susott, and D. E. Ward (1999), Trace gas emissions from laboratory biomass fires measured by Fourier transform infrared spectroscopy: Fires in grass and surface fuels, *J. Geophys. Res.*, *104*, 21,237–21,245.

Gras, J. L., J. B. Jensen, K. Okada, M. Ikegami, Y. Zizen, and Y. Makino (1999), Some optical properties of smoke aerosol in Indonesia and tropical Australia, *Geophys. Res. Lett.*, *26*(10), 1393–1396.

Guyon, P., B. Graham, G. C. Robers, O. L. Mayol-Bracero, W. Maenhaut, P. Artaxo, and M. O. Andreae (2003), In-canopy gradients, composition, sources and optical properties of aerosol over the Amazon forest, *J. Geophys. Res.*, *108*(D18), 4591, doi:10.1029/2003JD003465.

Hand, J. L., W. C. Malm, A. Laskin, D. Day, T. Lee, C. Wang, C. Carrico, J. Carrillo, J. P. Cowin, J. Collett Jr., and M. J. Iedema (2005), Optical, physical, and chemical properties of tar balls observed during the Yosemite Aerosol Characterization Study, *J. Geophys. Res.*, *110*, D21210, doi:10.1029/2004JD005728.

Hansen, A. D. A., H. Rosen, and T. Novakov (1984), The aethalometer—An instrument for the real-time measurement of optical-absorption by aerosol-particles, *Sci. Total Environ.*, *36*, 191–196.

Hoffer, A., A. Gelencsér, P. Guyon, G. Kiss, O. Schmid, G. Frank, P. Artaxo, and M. O. Andreae (2006), Optical properties of humic-like substances (HULIS) in biomass burning aerosols, *Atmos. Chem. Phys. Disc.*, *5*, 7341–7360.

Im, J.-S., V. K. Saxena, and B. N. Wenny (2001), An assessment of hygroscopic growth factors for aerosols in the surface boundary layer for computing direct radiative forcing, *J. Geophys. Res.*, *106*(D17), 20,213–20,224.

Kim, J., S.-C. Yoon, A. Jefferson, and S.-W. Kim (2006), Aerosol hygroscopic properties during Asian dust, pollution and biomass burning episodes at Gosan, Korea in April 2001, *Atmos. Environ.*, *40*, 1550–1560.

Kirchstetter, T. W., T. Novakov, and P. V. Hobbs (2004), Evidence that the spectral dependence of light absorption by aerosols is affected by organic carbon, *J. Geophys. Res.*, *109*, D21208, doi:10.1029/2004JD004999.

Kotchenruther, R. A., and P. V. Hobbs (1998), Humidification factors of aerosol from biomass burning in Brazil, *J. Geophys. Res.*, *103*(D24), 32,081–32,089.

Magi, B. I., and P. V. Hobbs (2003), Effects of humidity on aerosols in southern Africa during the biomass burning season, *J. Geophys. Res.*, *108*(D13), 8495, doi:10.1029/2002JD002144.

Malm, W. C., D. E. Day, S. M. Kreidenweis, J. L. Collett, and T. Lee (2003), Humidity-dependent optical properties of fine particles during the Big Bend Regional Aerosol and Visibility Observational Study, *J. Geophys. Res.*, *108*(D9), 4279, doi:10.1029/2002JD002998.

Malm, W. C., D. E. Day, S. M. Kreidenweis, J. L. Collett Jr., C. Carrico, G. McMeeking, and T. Lee (2005), Hygroscopic properties of an organic-laden aerosol, *Atmos. Environ.*, *39*, 4969–4982.

Patterson, E. M., and C. K. McMahon (1984), Absorption characteristics of forest fire particulate matter, *Atmos. Environ.*, *18*(11), 2541–2551.

Reid, J. S., R. Koppmann, T. F. Eck, and D. P. Eleuterio (2005a), A review of biomass burning emissions part II: Intensive physical properties of biomass burning particles, *Atmos. Chem. Phys.*, *5*, 799–825.

Reid, J. S., T. F. Eck, S. A. Christopher, R. Koppmann, O. Dubovik, D. P. Eleuterio, B. N. Holben, E. A. Reid, and J. Zhang (2005b), A review of biomass burning emissions part III: Intensive optical properties of biomass burning particles, *Atmos. Chem. Phys.*, *5*, 827–849.

Schmid, O., P. Artaxo, W. P. Arnott, D. Chand, L. V. Gatti, G. P. Frank, A. Hoffer, M. Schnaiter, and M. O. Andreae (2005), Spectral light absorption by ambient aerosols influenced by biomass burning in the Amazon Basin—1. Comparison and field calibration of absorption measurement techniques, *Atmos. Chem. Phys. Disc.*, *5*, 9355–9404.

Turn, S. Q., B. M. Jenkins, J. C. Chow, L. C. Pritchett, D. Campbell, T. Cahill, and S. A. Whalen (1997), Elemental characterization of particulate matter emitted from biomass burning: Wind tunnel derived source profiles for herbaceous and wood fuels, *J. Geophys. Res.*, *102*(D3), 3683–3699.

Weingartner, E., H. Saathoff, M. Schnaiter, N. Sreit, B. Bitnar, and U. Baltensperger (2003), Absorption of light by soot particles: Determination of the absorption coefficient by means of aethalometers, *J. Aerosol Sci.*, *34*, 1445–1463.

C. M. Carrico, Department of Atmospheric Science, Colorado State University, Fort Collins, CO 80523, USA.

D. E. Day and J. L. Hand, Cooperative Institute for Research in the Atmosphere, Colorado State University, Fort Collins, CO 80523, USA. (hand@cira.colostate.edu)

G. Engling, Research Center for Environmental Changes, Academia Sinica, Taipei 115, Taiwan.

W. C. Malm, National Park Service, Cooperative Institute for Research in the Atmosphere, Colorado State University, Fort Collins, CO 80523, USA.